Materials Physics and Chemistry (2018) Volume 1
doi:10.24294/mpc.v1i1.356

Template Assisted Nano-Structured Nickel for Efficient Methanol Oxidation

S. Mohanapriya Subramanian, V Raj

Advance Materials Research Lab, Department of Chemistry, Periyar University, Salem-636 011, India

ABSTRACT

Nanoporous Nickel has been prepared by electrodeposition using non-ionic surfactant based liquid crystalline template under optimized processing conditions. Physico-chemical properties of Nanoporous nickel is systematically characterized through XRD, SEM and AFM analyses. Comparison of electrocatalytic activity of Nanoporous nickel with smooth nickel was interrogated using cyclic voltammetry (CV), chronoamperometry (CA) and electrochemical impedance spectroscopy (EIS) analyses. Distinctly enhanced electrocatalytic activity with improved surface poisoning resistance related to Nanoporous nickel electrode towards methanol oxidation stems from unique Nanoporous morphology. This Nanoporous morphology with high surface to volume ratio is highly beneficial to promote active catalytic centers to offer readily accessible Pt catalytic sites for MOR, through facilitating mass and electron transports.

***Keywords*:** Template Deposition; Electrocatalysis; Methanol Oxidation; Direct Methanol Fuel Cell

1. Introduction

Owing to the simplified system design, high energy density and ease of transportation of fuel, Direct methanol fuel cells (DMFCs) are currently at forefront as renewable energy sources which involves electrochemical energy conversion and hence suitable for automotive as well as portable power applications[1-4]. Till now, Platinum (Pt) and its alloys represent most extensively used DMFC electrocatalysts on account of their superior catalytic activity and stability towards oxidation of methanol at anode side[5-7]. But catalytic activity of Pt surface could easily deteriorated by the adsorption of CO generated during methanol oxidation reaction (MOR).

Promoting effect of Ni over Pt catalytic activity both in acidic and alkaline medium is well established in literature[8-10]. Earlier studies established the role of nickel in assisting the dissociative adsorption of water molecules to produce-OHads species, which facilitates the oxidation of CO adsorbed on Pt surface thereby favors regeneration of Pt catalytic centers. Many electrodes involving nickel as a component in their manufacture can be used as catalysts in fuel cells. It is commonly used as an electro-catalyst for both anodic and cathodic reactions in organic synthesis and water electrolysis[15–18]. One of the very important uses of nickel as a catalyst is for the oxidation of alcohols. Several studies of the electro-oxidation of alcohols on nickel have been reported. Alkaline direct methanol fuel cells are now receiving considerable attention because they allow the use of anion exchange membranes that reduce methanol cross-over – a serious problem with cation exchange membrane used in acidic methanol fuels[8]. Another reason for using alkaline medium is because the kinetics for both methanol oxidation and oxygen reduction reactions is found to be more facile in alkaline medium than in acidic one[9-12]. In recent years, the focus of research is towards finding cheaper alternative electrocatalysts and improving the overall cell performance. Non noble transition metal electrocatalysts such as copper[13-16], nickel[17-24] which oxidise methanol and other alcohols, offer good alternative electrocatalysts. The activity of nickel based electrocatalysts depends on the method of preparation of these electrodes. Rahim et al.,[24] showed that only nickel dispersed in graphite is catalytically active for methanol oxidation while massive nickel is not. Also this nickel electrocatayst, after continuous cycling loses its performance due to possible loss of activity of nickel oxide[24]. This is believed to be due to increased thickness of NiO(OH) which acts as a barrier inhibiting the charge transfer

doi: 10.24294/mpc.v1i1.356

process for methanol oxidation. Alternative approaches to the preparation of nickel electrocatalysts that can minimise the buildup of such a barrier layer, would be of great interest in the development of non-noble metal electrodes for methanol oxidation.

The purpose of the present work is to establish the electro-catalytic oxidation of methanol on Nanoporous nickel in a solution of 1.0 M NaOH. Surfactant mesophases come under the category of soft template systems and electrodeposition through them is a very useful and versatile method for the synthesis of nanostructured materials. In addition, lyotropic liquid crystalline phases possess a long-ranged spatially periodic architecture with lattice parameters in the range of a few nanometers. This makes them ideal candidate systems for synthesis of nanomaterials. In this study, we report a simple electrochemical method of preparing a high surface area Nanoporous nickel deposit, using a new hexagonal liquid crystalline phase as template. This room temperature deposited nickel has been characterized by electrochemical techniques such as cyclic voltammetry (CV) and electrochemical impedance spectroscopy. Besides, scanning electron microscopy (SEM), Atomic force microscopy (AFM) and X-ray diffraction (XRD) are also used for surface characterization. Catalytic efficiency of synthesized Nanoporou s nickel is evaluated by methanol oxidation using the techniques such as CV, Impedance etc., Morphology and composition of Nanoporous nickel cloud easily be tuned through controlling parameters involved in electrodeposition.

2. Experimental

2.1 Chemicals

Triton X-100 (Spectrochem), Poly(acrylic acid) (PAA) (Aldrich), sodium hydroxide pellets (Emerck), nickel(II) chloride (EMerck), nickel sulphamate (Grauer and Wheel), boric acid (Sarabhai chemicals) were used in this study. All chemical reagents used were AnalaR (AR) grade. Millipore water having a resistivity of 18 M cm was used in all the experiments.

2.2 Preparation and characterization of hexagonal liquid crystalline phase

Hexagonal liquid crystalline phase was prepared from a ternary mixture of Triton X-100, poly(acrylic acid) and water. We have carried out our studies at two different weight compositions viz. (1) Triton X-100 42% + water 58%. The mixture was stirred in a magnetic stirrer at a temperature of 33–35◦ C for 1 h and was allowed to cool down to room temperature. When viewed under a polarized light microscope, the mixture shows the characteristic birefringence of a hexagonal liquid crystalline phase stable up to 29° C. All the electrodeposition using this phase as template has been done at the room temperature of 25°C.

2.3 Nickel electroplating through hexagonal liquid crystalline

The electrodeposition of Nanoporous nickel was performed in a standard three-electrode glass cell using Al as a working electrode, a saturated calomel electrode (SCE) and Pt foil served as a reference and counter electrodes respectively. Nanoporous nickel was synthesized through electrodeposition at a constant of -1 V for different time period. For electrodeposition, we have prepared the aqueous phase of the above described hexagonal liquid crystalline system from the standard nickel sulphamate bath[21] of the composition: 300 g l^{-1} nickel sulphamate, 6 g l^{-1} nickel chloride and 30 g l^{-1} boric acid.

3. Results and discussion

3.1 Micro-structural analyses

Interesting electrocatlytic properties is exhibited by mesooporous nickel owing to their high surface area, unique morphology and high conductivity. Schematics of synthesis of steps involved in the process of preparation of Nanoporous nickel is illustrated in **Figure 1.** Triton X 100 forms micelles aggregated in the aqueous phase. Nickel ions encapsulated in the micelles of Triton X100 undergoes electrochemical reduction in such way that meso domains are created over the surface. Textural properties of nickel deposit are modified due to entrapment of nickel ions inside the micelles.

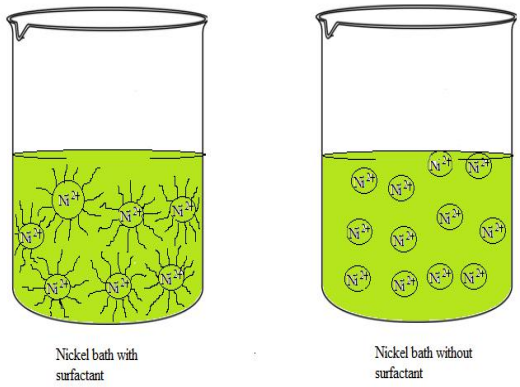

Figure 1a; Pictorial representation of nickel bath with and without surfactant**.**

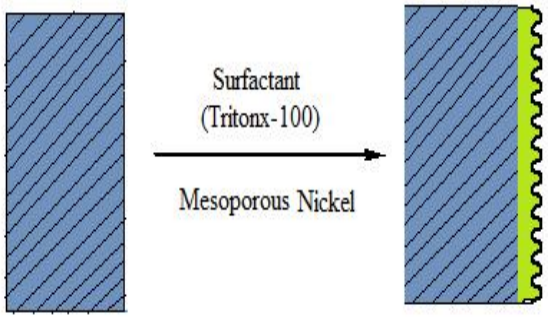

Figure 1b; Schematic representation for preparation of Nanoporous nickel**.**

Nanoporous nickel was characterized by X-ray powder diffraction (XRD). It can be noticed from **Figure 2** that XRD pattern of nickel deposited electrodes clearly reveal the characteristic peaks expected for nickel with face centered cubic (fcc) structure in addition to the reflections observed for bare Al electrode. Nanoporous nickel deposited show the peaks at 44.3^o and 51.8^o corresponding to (111) and (200) planes respectively and are indicated by the asterisk mark in the figure. The ratio of intensities of (111) and (200) planes associated with these nickel electrodes with and without surfactant suggests that there is a preferential growth and orientation of nickel film along (200) direction in the case of surfactant electro deposition. It can be noticed from the figure that XRD pattern of nickel deposited electrodes clearly reveal the characteristic peaks expected for nickel with face centered cubic structure.

SEM pictures of nickel deposited on with and without addition of Triton-X 100 are provided in **Figure 3.** The morphology of an individual deposit depends upon the electrolyte used for deposition. These images clearly display the distinguishable structural features indicating the homogeneous growth of nickel deposits. In effect, template deposited Nickel exhibits a higher amount of uniform growth compared to the nickel electrode produced without the template.

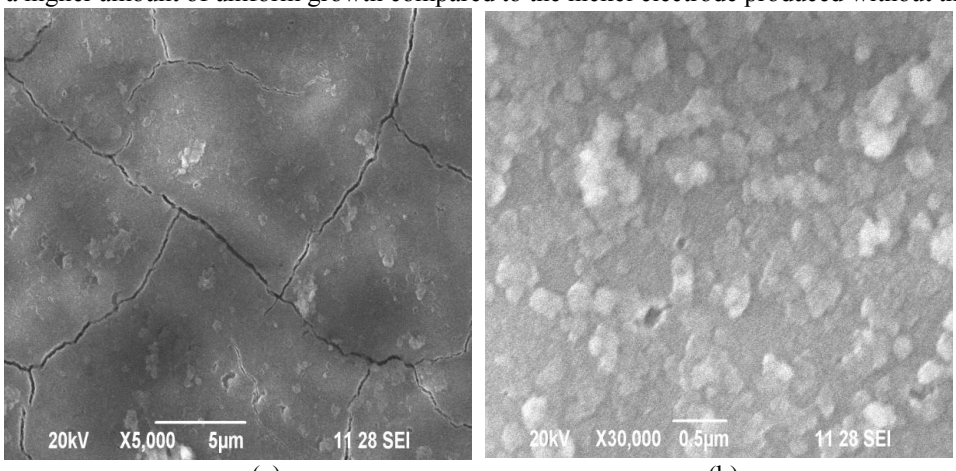

(a) (b)

Figure 3; SEM images of (a) Nanoporous nickel and (b) Smooth nickel**.**

The particles are same-sized spheres with smooth surfaces, the surface area can be related to the average equivalent particle size by d =6000/(ρ.s) (in nm), where d is the average diameter of spherical particle in manometer; ρ is the theoretical density of nickel (g/cm^3) and s represents the measured surface area of the powder in m^2/g. The size of the particles are in the range of 5- 10 μm. Compare to the both images Nanoporous nickel surface morphologies presents higher roughness.

AFM studies also validate the above observation as presented by **Figure 4.** AFM studies are used to demonstrate the difference in topography of Nanoporous nickel and smooth nickel. Difference in the surface topographies related to Nanoporous

nickel and smooth nickel are evaluated through AFM analysis. Nanoporous structure helps to improve electronic conductivity which is highly advantageous for efficient electrocatalysis. The modulations in the height profile indicate that synthesized Nanoporous nickel is associated with high degree of roughness. Surface modulations on the Nanoporous nickel drastically increase the roughness factor associated with it, however nickel deposited using electrolyte bath without addition of surfactant exhibits two times lower roughness.

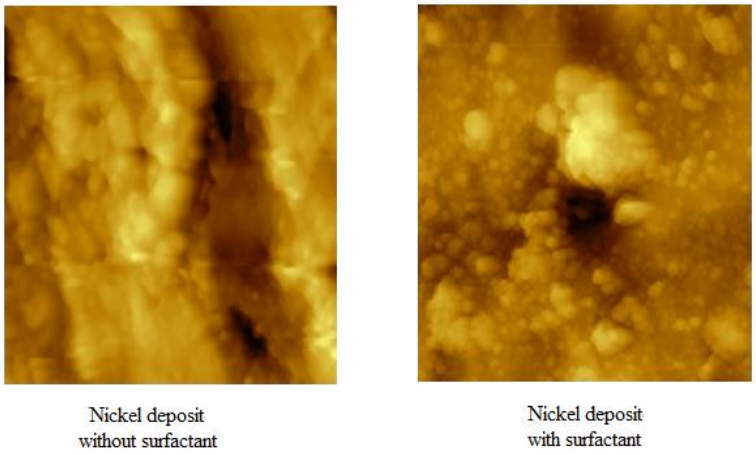

Figure 4; AFM images of smooth nickel and Nanoporous nickel**.**

It is because of this unique porous structure eletrocatalytic activity of Nanoporous nickel is higher. Distinct porous structure of Nanoporous deposits, which substantially increase the surface area. SEM and XRD studies are in good agreement with AFM results.

3.2 Electrochemical studies

The electrochemical activity of mseoporous nickel electrode was studied by Cyclic Voltammetry, Amperometry and Electrochemical Impedance techniques. The cyclic voltammograms (CV) of nickel deposited with and without the addition of Triton-X100 were recorded in alkaline medium. The CV measurements were conducted in 0.1 M NaOH at scanning rate of 100 mV/s. The applied potential was limited between 1 and -1V.

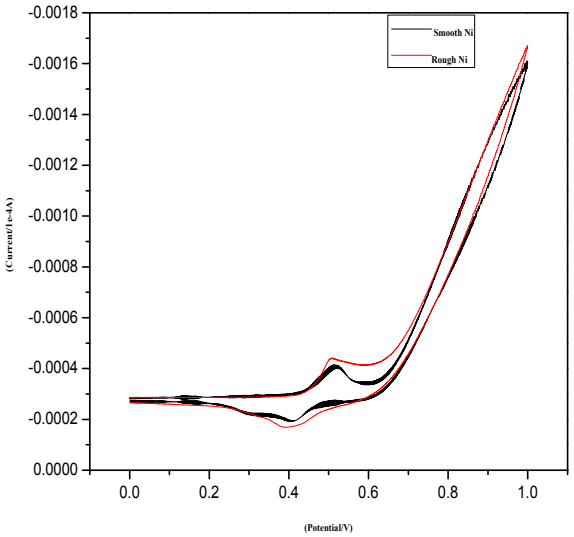

Figure 5; Cyclic Voltametry curves of Nanoporous nickel and smooth nickel scanned from -1V to 1V at a scan rate of 50 mV/s performed in 0.1M NaOH**.**

When discussing the electrochemical behavior of nickel, it is convenient to consider the three oxide phases formed when a positive potential is applied to the metallic nickel electrode. A cyclic voltametry (CV) profile of nickel in aqueous alkaline solution reveals features corresponding to the formation of three oxide species as the potential is increased from –1 to 1 V vs hydrogen evolution reaction. The anodic peak corresponding to the formation of the first

surface oxide, α-$Ni(OH)_2$, is present in the V range of –1to 1 V. If the CV scan is reversed at a potential lower than 0.50 V, the full reduction of α-$Ni(OH)_2$ to metallic nickel will occur, giving rise to a cathodic peak in the CV profile at $-1 \leq E \leq 1$ V . When the potential is brought to values lower than 0.00 V, appreciable current density as a result of the hydrogen evolution reaction (HER) is observed along with the formation of H_2 (gas) bubbles at the electrode. The HER overlaps in potential with the reduction of α-$Ni(OH)_2$. If the forward CV scan is continued to potentials higher than 0.50 V, the α-$Ni(OH)_2$ already present on the electrode is converted to β- $Ni(OH)_2$, and additional β-$Ni(OH)_2$ is formed. This species is formed in the E region between 0.50 V and 1.30 V, which is known as the passive potential region for nickel. Of these two $Ni(OH)_2$ structures, the β phase is more stable. Formation of this phase is irreversible, meaning that β-$Ni(OH)_2$ cannot be removed from the surface of the electrode by simply reversing the potential and reducing the oxide electrochemically. Once formed, β-$Ni(OH)_2$ can be removed through chemical etching, mechanical polishing, and thermal reduction in a hydrogen environment. The α and β $Ni(OH)_2$ species have different crystallographic structures; the α phase incorporates either water or alkali cations from the electrolyte and has a lattice constant that is larger than that of β-$Ni(OH)_2$. The final oxidation species to be formed is NiOOH. at E > 1.30 V; the β-$Ni(OH)_2$ species is oxidized reversibly to β-NiOOH which has a similar crystallographic structure and lattice constant. If an increasing positive potential is continuously applied, a γ-NiOOH phase is formed. This species adopts a crystallographic structure similar to that of α-$Ni(OH)_2$ and can be electrochemically reduced back to β-$Ni(OH)_2$.

From **Figure 5** it is evident that Nanoporous nickel deposits presnts higher current density compared to smooth nickel prepared without asddition of surfactant. It has been reported that periodic Nanoporous structures with high surface area can have charge storage capacity by one order over that of the bulk materials. Increased electrochemical surface area of Nanoporous deposits are due to presence of Triton-X100 molecules during deposition porcess. These surfactant molecules acts as a template during deposition, creates mesopores in the nickel surface and favors the formation of highly acctive Nanoporous nickel deposits. Owing to the larger surface area elelctrochemically actvie surface area is alos higher for the Nanoporous nickel deposits.

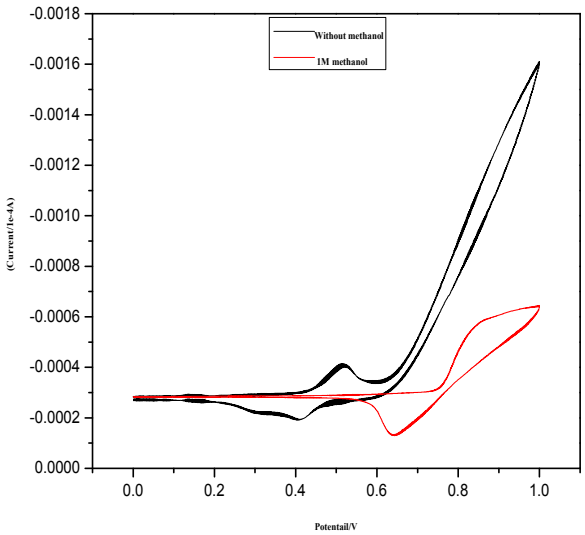

Figure 6; Cyclic voltametric curves of smooth nickel without and with 1M methanol scanned from -1V to 1V at a scan rate of 50 mV/s performed in 0.1M NaOH**.**

Higher roughness associated with mesopores nickel is due to the lagere number of electrolyte accessing channels formed over Nanoporous nickel due to more avalibility of electrolyte acess-electrochemical surface area. In other words through the Nanoporous deposits, electrolyte could easily reach the nickel surface compared to smooth nickel.

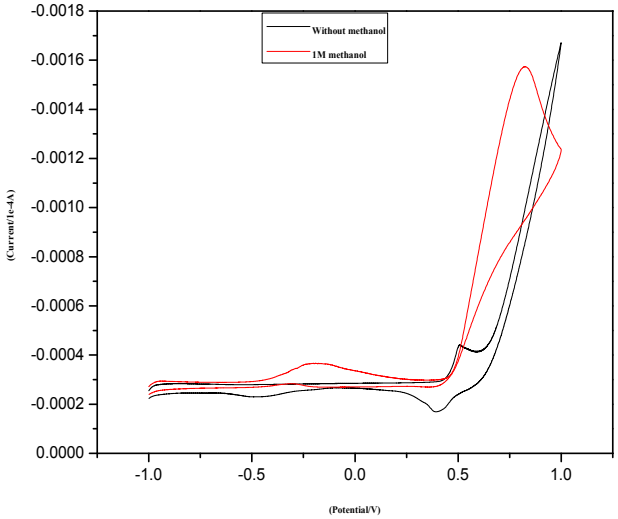

Figure 7; Cyclic Voltametric curves of Nanoporous nickel without and with 1M methanol scanned from -1V to 1V at a scan rate of 50 mV/s performed in 0.1M NaOH**.**

Electro catalytic response of prepared nickel deposits are evaluated through the addition of 1 M methanol. CV curves of nickel deposits before and after addition of 1M methanol in 0.1 M aqueous NaOH solution are given in **Figure 6** and **Figure 7** respectively. Since NiOOH was constantly being reduced back to $Ni(OH)_2$ once methanol oxidation started, some anodic current could always be attributed to the continuous re-oxidation of $Ni(OH)_2$ back to NiOOH. Furthermore, during the cathodic scans, lingering methanol oxidation caused some portion of the electrode surface to be prematurely reduced to the Ni^{2+} oxidation state before the Ni^{3+}/Ni^{2+} reduction occurred, thus decreasing the amount of NiOOH on the surface and the magnitude of the corresponding peak. On comparing electro catalytic response of methanol on Nanoporous nickel and smooth nickel, it is clear that anodic peak current associated with methanol electro oxidation is higher for Nanoporous nickel. Increase in the anodic peak current on the addition of 1 M methanol is 0.0012 mA/cm^2 and 0.0002 mA/cm^2 for Nanoporous nickel and smooth nickel respectively. Improved current response clearly demonstrates significance of Nanoporous structure.

The onset of methanol oxidation occurs at about 500 mV at Nanoporous nickel electrode whereas methanol oxidation begins from 550 mV with smooth nickel electrode. The lower onset potential associated with Nanoporous nickel clearly evidences higher electro catalytic activity for MOR. Superior catalytic activity of Nanoporous nickel may stem from unique porous morphology associated with higher ESCA. It is evident that peak potential at which methanol oxidation occurs on Nanoporous nickel is 0.75 V but it is 0.85 V for smooth nickel.

As well known, the forward current peak (I_f) is attributed to the oxidation of methanol molecule and the backward current peak (I_b) to the oxidation of adsorbed intermediates such as CO, CHxOH ($0 < x < 2$), CHxO, $HCOO^-$ and so on. Hence, amount of oxidizable intermediates adsorbed over the catalytic surface could be predicted by the relative magnitude of backward peak. $(I_f)/(I_b)$ ratio is a measure of efficiency of a catalyst to tolerate towards poisoning of surface due to adsorption of incompletely oxidized intermediates. $(I_f)/(I_b)$ value for Nanoporous nickel and smooth nickel is 1.3 and 1.17 respectively, which are higher than that of pure Pt as reported earlier. Higher $(I_f)/(I_b)$ value indicates that most of the intermediate carbonaceous species were oxidized to carbon dioxide in the forward scan on Nanoporous nickel electrode. Increased CO tolerance of Nanoporous nickel electrode may be attributed due to basic difference in methanol oxidation between Nanoporous and nonporous structure, which could be explained on the basis of morphology dependant CO tolerance as demonstrated earlier. Based on the results, it could be inferred that Nanoporous architecture increases poisoning tolerance of the catalyst through influencing the availability of continuous binding sites for C-H bond cleavage and enhances more number of readily accessible active catalytic sites for methanol oxidation reaction (MOR). The schematic illustration of mechanism of CO removal over Nanoporous nickel is depicted in **Figure 8.**

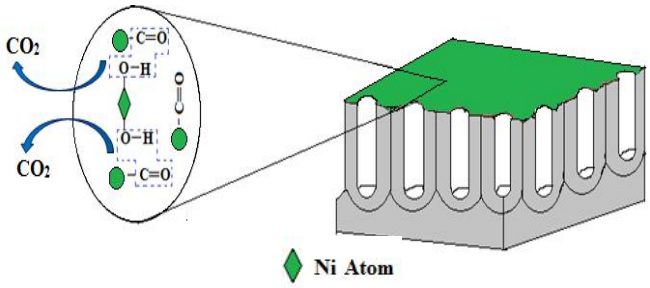

Figure 8; Mechanism of electro-oxidation of methanol on Nanoporous nickel catalyst**.**

Various concentration of methanol 2M, 3M, 4M, and 5M were added to smooth nickel and Nanoporous nickel. Smooth nickel has good electro catalytic activity, but surfactant Tritonx-100 nickel has high electro catalytic activity **Figure 9** and **Figure 10** respectively.

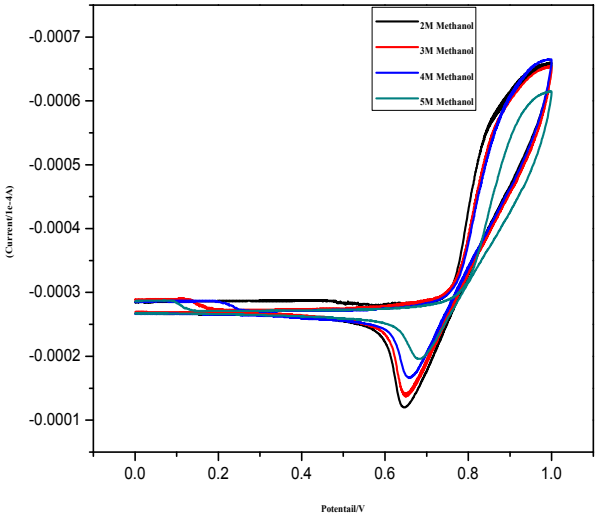

Figure 9; Cyclic Voltametric curves of smooth nickel in various concentration of methanol scanned from -1V to 1V at a scan rate of 50 mV/s performed in 0.1M NaOH**.**

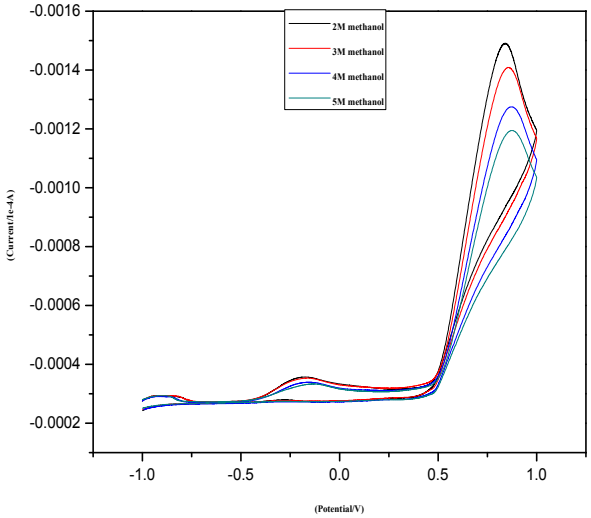

Figure 10; CV curves of Nanoporous nickel in various concentration of methanol scanned from -1V to 1V at a scan arte of 50 mV/s performed in 0.1M NaOH**.**

CV was used to examine the electrochemical properties of Nanoporous nickel in aqueous alkaline electrolyte and

to relate such acquired insight to their chemical composition and surface characteristics. A typical CV curves for bulk nickel in aqueous NaOH solution in the –1 to +1 V potential (E) range shows the following anodic features: (i) oxidation of metallic nickel to α-$Ni(OH)_2$ at $0.20 < E < 0.40$ V (ii) concurrent conversion of α-$Ni(OH)_2$ to β-$Ni(OH)_2$ and oxidation of metallic nickel to β-$Ni(OH)_2$ at $0.50 < E < 1.30$ V; (iii) increase of the oxidation state of Ni from +2 to +3 through the oxidation of β-$Ni(OH)_2$ to β- NiOOH at $1.30 < E < 1.55$ V and (iv) oxygen evolution reaction (OER) at $E \geq 1.55$ V. The β phase of $Ni(OH)_2$ is the most stable and thermodynamically favored oxide of nickel; it is the passive layer that develops on the surface of metallic nickel upon contact with the ambient environment. The conversion of α-$Ni(OH)_2$ to β-$Ni(OH)_2$ is irreversible and once it has taken place, the cathodic peak corresponding to the reduction of α -$Ni(OH)_2$ is not observed anymore. The reduction of β-$Ni(OH)_2$ cannot be accomplished electrochemically and can be achieved at elevated temperatures in the presence of $H_2(g)$. The anodic and cathodic peaks characteristic of α-$Ni(OH)_2$ formation and reduction are not observed because a layer of β-$Ni(OH)_2$ has developed as the result of several prior CV scans. The CV curves for nickel Nanoporous displays the same features as those observed for smooth nickel in alkaline media. The CV curves for Nanoporous nickel reveals pronounced differences as compared to the CV curves for smooth nickel, especially in the anodic scan. Compared to the mesporous nickel, the peak is shifted towards higher potentials and overlaps the region of OER. The value of Is for OER is greater than in the case of nickel Nanoporous; the specific current for the cathodic feature is greater than in the case of nickel Nanoporous but the difference is small. Nickel and Nanoporous nickel have very different surface morphologies and the rough, bubbly surface of Nanoporous nickel gives rise to a larger surface area than smooth nickel. The charges under the two cathodic peaks are similar, thus indicating that both samples have similar amounts of β-NiOOH on the surface. Bearing in mind that the difference in Qs values for smooth nickel is less than 40% and that Nanoporous nickel has a significantly larger real surface area, we conclude that β-NiOOH does not make up the entire surface of Nanoporous nickel.

3.3. Chronoamperometry

In order to evaluate the long term activity of the catalyst, the steady state current responses of Nanoporous nickel and smooth nickel were recorded.

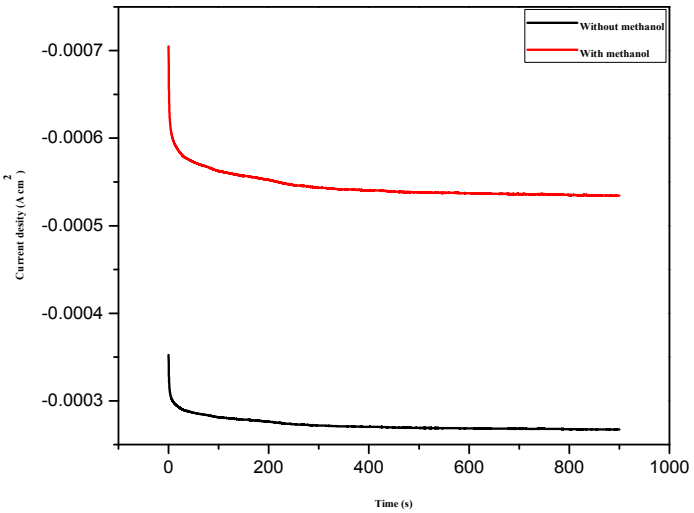

Figure 11; Amperometric curves of using Nanoporous nickel without and with 1M methanol**.**

Initial rapid current decay for the both catalysts is due to double layer capacitance. Transient current due to methanol oxidation attains a steady state after 820 s and 1600 s with Nanoporous nickel electrode and smooth nickel electrode respectively, indicating better catalytic performance of the former. It could be noticed from chronoamperometric results that addition of 1M methanol shows an increased electrocatalytic response on Nanoporous nickel surface but increase current response is not very high with smooth nickel. As evident from the figures addition of 1M methanol causes increase in current 0.07 A/cm^2 with Nanoporous nickel and it is 0.0001 mA/cm^2 for smooth nickel.

Methanol oxidation current tends to decrease due to the accumulation of adsorbed species on catalyst surfaces due

to the decomposition of methanol molecules. On comparing the current responses, it is obvious that Nanoporous nickel electrode possesses enhanced catalytic durability. Unique Nanoporous structure comprising continuous Meso channels is highly favorable to provide easy transport paths of electrons and reaction intermediates therefore enhances MOR activity of Nanoporous nickel electrode.

3.4. Impedance studies

To further extract information about the electro catalytic process, EIS studies are performed. **Figure 12** and **13** represent Nyquist plots recorded at 500 mV dc-offset potential in 0.1 M NaOH with methanol for Nanoporous nickel and smooth nickel electrodes respectively.

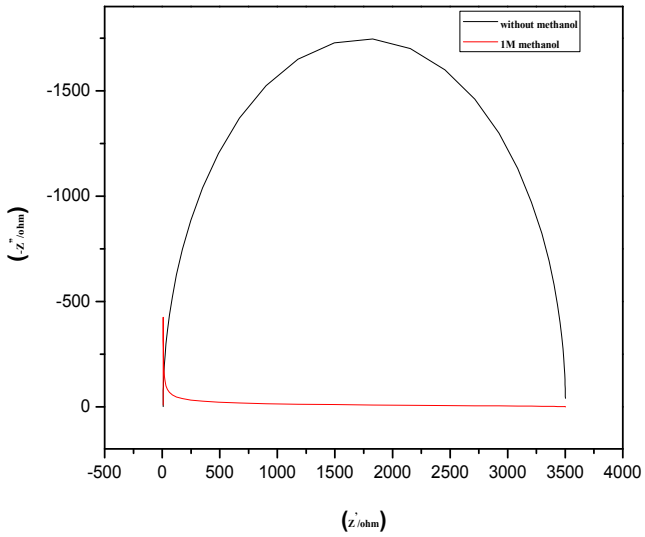

Figure 12; Impedance of Nanoporous nickel deposition, without and with 1M methanol**.**

General pattern of Nyquist plot obtained with electrodes under study is unaltered on changing the concentration of methanol from 0.1 to 4 M, pointing that mechanism of methanol oxidation is not affected by methanol concentration. Conversely, diameter of semicircle has been dramatically decreased on increasing the concentration of methanol denoting that charge transfer resistance (R_{ct}) regularly drops.

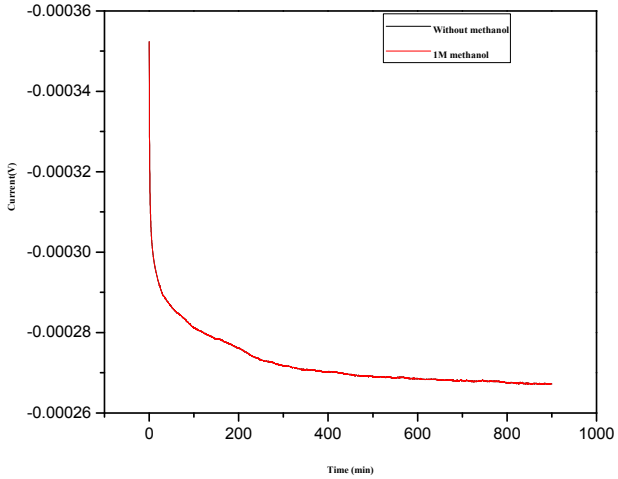

Figure 13; Impedance of smooth nickel deposition, without and with 1M methanol**.**

EIS analysis was carried out by fitting the data with appropriate equivalent circuit as shown in Table-1. Equivalent circuit is composed of solution resistance (R_s), double layer capacitance (CPE_1) and charge transfer resistance (R_{ct}) associated with MOR. Porous nature of electrode is attributed by the presence of additional elements namely CPE_2 and R_f. The values for all the parameters R_{ct}, CPE_1, CPE_2, and their associated % error determined by the fitting of the experimental EIS data are summarized in **Table 1** and **2**. The parallel combination of the charge-transfer resistance (R_{ct})

and CPE take into account for methanol adsorption and oxidation on porous thin film.

R_s/Ω^{-1}	$CPE_1(\times10^6)/\Omega^{-1}s^n$	n_1	R_{ct}/Ω^{-1}	$CPE_2(\times10^5)/\Omega^{-1}s^n$	n_2	R_f/Ω^{-1}	Concentration of Methanol (M)
14.8	4.186	0.91	1866.7	9.93	0.92	32380	0
12.78	5.636	0.87	875.8	7.95	0.94	632.7	1
11.65	6.10	0.88	153.3	4.28	0.91	449.7	2
11.5	2.68	0.92	102.2	2.998	0.93	427.2	3
11.58	4.22	0.96	82.2	1.746	0.89	499.1	4

Table 1. Numerical values of elements in the equivalent circuit fitted with Nyquist plots of Nanoporous nickel

R_s/Ω^{-1}	$CPE_1(\times10^6)/\Omega^{-1}s^n$	n_1	R_{ct}/Ω^{-1}	$CPE_2(\times10^5)/\Omega^{-1}s^n$	n_2	R_f/Ω^{-1}	Concentration of Methanol (M)
15.1	5.767	0.88	3381.9	2.5	0.89	89342	0
15.02	3.761	0.89	1505	4.536	0.9	6861.4	1
12.5	2.504	0.85	771.4	3.089	0.91	739.5	2
12.3	5.766	0.91	537.8	5.292	0.89	324.8	3
12.32	4.34	0.89	331.7	4.7	0.95	241.9	4

Table 2. Numerical values of elements in the equivalent circuit fitted with Nyquist plots of smooth nickel

The parallel combination R_{ct} with CPE leads to a depressed semicircle in the corresponding Nyquist impedance plot. It is noteworthy that R_{ct} is an order lower for Nanoporous nickel than that of smooth nickel, which reflects the enhanced electro catalytic activity of the former. The Electrochemical Impedance spectroscopic (EIS) has a power tool for studying the electrochemical behavior of electrode.

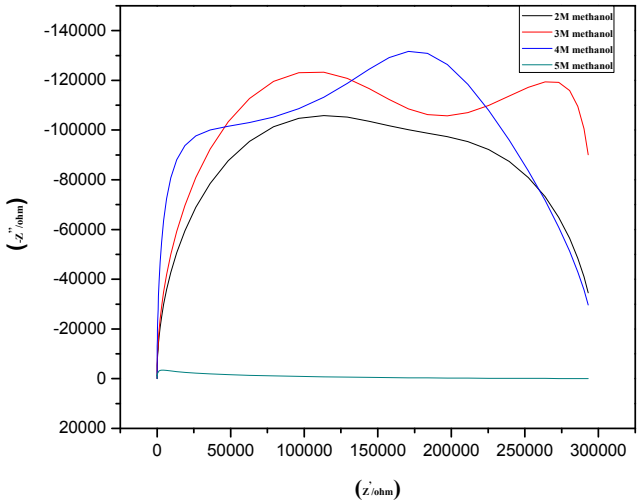

Figure 14; Impedance of smooth nickel deposition, 2M, 3M, 4M, and 5M methanol**.**

Figure 12 and **13** It can be seen that the R_{ct} values are found to decrease in the order 1M methanol > without methanol. Without methanol is low resistance compared to 1M methanol. The diameter of the semicircle is proportional to the value of the impedance. The smaller the value of impedance, the better will be the conducting property of the coating. This can be further confirmed by its low resistance and high capacitance.

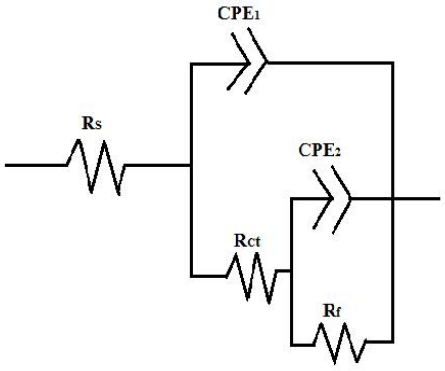

Likewise the equivalent circuit shown **Figure 13** is a simplified electrochemical model which has been used to fit the impedance data obtained for the composite coatings present on substrate. As seen from the equivalent circuit, R_s

refers to the resistance of the solution, C_{dl} is the electric double layer capacitance and R_{ct} is the charge transfer resistance that represents the electrochemical activity of the electrode. Based on equivalent circuit model proposed, these EIS curves were best fitted.

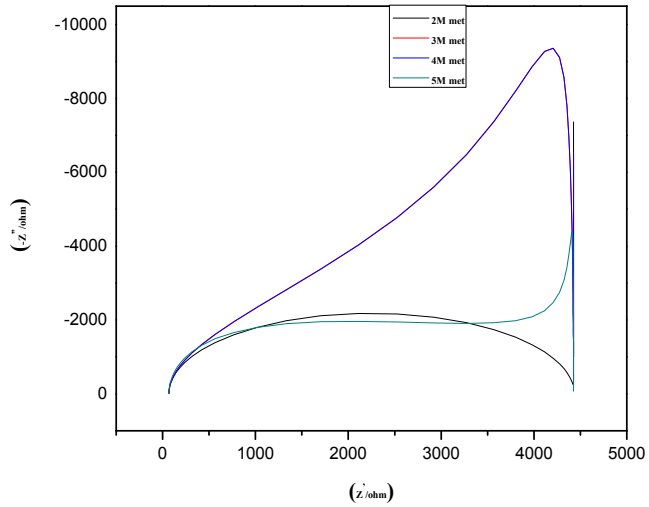

Figure 15; Impedance of Nanoporous nickel deposition with 2M, 3M, 4M, and 5M methanol**.**

Various concentration of methanol solution in Tritonx-100 surfactant the deposited nickel has low resistance and high capacitance.

4. Conclusions

In a nutshell, a facile and simple approach is adopted the produce Nanoporous nickel through electrodeposition using surfactant Triton-X100. The developed methods is scalable and reproducible Triton-X100 template could be easily removed by washing the electrode with water. Nanoporous nickel has been prepared by surfactant assistant assisted electrochemical deposition of nickel under optimized process conditions. Surface characteristics of the Nanoporous nickel and smooth nickel were systematically characterized through XRD, SEM, and AFM analyses. Nanoporous morphology is highly beneficial to offer readily accessible catalytic sites for methanol oxidation reaction (MOR), through facilitating mass and electron transport. The prepared nickel was used as electrocatalyst for DMFC. Comparison of electrocalytic activity of Nanoporous nickel with smooth nickel was interrogated using cyclic voltammetry (CV), chronoamperometry (CA) and electrochemical impedance spectroscopy (EIS) analyses. Distinctly enhanced electrocatalytic activity with improved CO tolerance associate with Nanoporous nickel electrode towards methanol oxidation stems from readily accessible high surface area associated with Nanoporous structured, which facilitate mass transport of both the reactants and products.

Acknowledgements

One of the authors S. Mohanapriya is grateful to University Grants Commission (UGC), Government of India, for providing fund under the scheme of ‘UGC-Dr. D. S. Kothari Post Doctoral Fellowship’. (Ref: No. Award Letter-No.F.4-2/2006 (BSR)/CH/14-15/0102 dated 5-5-2015).

References

1. Liu H, Song C, Zhang L, Zhang J, Wang H and Wilkinson D P 2006 J. Power Sources 155 95.
2. Neburchilov V, Martin J, Wang H and Zhang J 2007 J. Power Sources 169 221.
3. Mohanapriya S, Sahu A K, Bhat S D, Pitchumani S, Sridhar P and Shukla A K 2009 Energy Environ.Sci. 2 1210.
4. Mohanapriya S, Bhat S D, Sahu A K, Manokaran A, Vijayakumar R, Pitchumani S, Sridhar P and Shukla A K 2010 Energy Environ. Sci. 3 1746.
5. Mohanapriya S, Sahu A K, Bhat S D, Pitchumani S, Sridhar P, George C, Chandrakumar N and Shukla A K 2011 J. Electrochem. Soc. 158 A1.
6. Mohanapriya S, Bhat S D, Sahu A K, Manokaran A, Pitchumani S, Sridhar P and Shukla A K 2009 J. Bionanoscience 3 131.
7. Suganthi S, Mohanapriya S and Raj V 2016 J. Appl. Polym. Sci. 133 43514.

8. Iwasita T 2007 Electrochim. Acta 47 3663.
9. Radmilovic V, Gasteiger H A and Ross P N 1995 J. catal. 154 98.
10. E. Antolini E, Jose, Salgado R C and Gonzalez R 2006 Applied Catalysis B: L Environmental 63 137.
11. Wasmus S and Kuver A 1999 J electroanal. Chem. 461 14.
12. Iwasita T, Hoster H, John-Anacker A, Lin W F and Vielstich W 2000 Langmuir 16 522.
13. Wang K, Gasteiger H A, Markovic N M and Ross P N 1996 Electochim. Acta 41 2587.
14. Hu Y, Zhang H, Wu P, Zhou H and Cai C 2011 Phys. Chem. Chem. Phys. 13 4083.
15. Liu X J, Cui C H, Gong M, Li H H, Xue Y, FanF J and Yu S H 2013 Chem. Commun. 49 8704.
16. Xu D, Liu Z, Yang H, Liu Q, Zhang J, Fang J, Zou S and Kai Sun 2009 Angew. Chem. Int. Ed. 48 4217.
17. Mohanapriya S, Suganthi S and Raj V 2017 J. Porous Mater. 24 355.
18. Abdel Rahim M A, Hassan H B and Abdel Ham R M 2007 Fuel cells 4 298.
19. Niu Z, Wang D, Yu R, Penga Q and Li Y 2012 J. Chem. Sci. 3 1925.
20. Ganesh V and Lakshminarayanan V 2004 Electrochimi. Acta 49 3561.
21. Xia Y, Xiong Y, Lim B and SkrabalakS E 2009 Angew. Chem. Int. Ed. Engl. 48 60.
22. Mohanapriya S, Tintula K K, Bhat S D, Pitchumani S and Sridhar P 2012 Bull. Mater. Sci. 35 297.
23. Julia van D, Brandy Kinkead P, Yoseif M and Gregory J 2014 ACS Appl. Mater. Interfaces 6 15.
24. Mohanapriya S, Suganthi S and Raj V 2017 J. Porous Mater. 24 355.
25. Xing W, Li F, Yan Z F and Lu G Q 2004 J. Power Sources 134 324.
26. Skowronski J M and Wazny A 2006 J. New Mater. Electrochem. Syst. 9 345.
27. Abdel rahim M A, Abdel Hameed R M and Khalil M W 2004 J. Power sources 134 160.